

## Lifetime measurement of the first excited $2^+$ state in $^{112}\text{Te}$

M. Doncel,<sup>1</sup> T. Bäck,<sup>1</sup> D. M. Cullen,<sup>2</sup> D. Hodge,<sup>2</sup> C. Qi,<sup>1</sup> B. Cederwall,<sup>1</sup> M. J. Taylor,<sup>2</sup> M. Procter,<sup>2</sup> K. Auranen,<sup>3</sup> T. Grahn,<sup>3</sup> P. T. Greenlees,<sup>3</sup> U. Jakobsson,<sup>1,3</sup> R. Julin,<sup>3</sup> S. Juutinen,<sup>3</sup> A. Herzán,<sup>3</sup> J. Konki,<sup>3</sup> M. Leino,<sup>3</sup> J. Pakarinen,<sup>3</sup> J. Partanen,<sup>3</sup> P. Peura,<sup>3</sup> P. Rahkila,<sup>3</sup> P. Ruotsalainen,<sup>3</sup> M. Sandzelius,<sup>3</sup> J. Sarén,<sup>3</sup> C. Scholey,<sup>3</sup> J. Sorri,<sup>3</sup> S. Stolze,<sup>3</sup> and J. Uusitalo<sup>3</sup>

<sup>1</sup>Royal Institute of Technology, 10691 Stockholm, Sweden

<sup>2</sup>School of Physics and Astronomy, Schuster Laboratory, The University of Manchester, Manchester M13 9PL, United Kingdom

<sup>3</sup>University of Jyväskylä, Department of Physics, P. O. Box 35, FI-40014 University of Jyväskylä, Finland

(Received 15 April 2015; revised manuscript received 25 May 2015; published 23 June 2015)

The lifetime of the  $2^+ \rightarrow 0^+_{\text{g.s.}}$  transition in the neutron-deficient nucleus  $^{112}\text{Te}$  has been measured for the first time using the DPUNS plunger and the recoil distance Doppler shift technique. The deduced value for the reduced transition probability is  $B(E2 : 0^+_{\text{g.s.}} \rightarrow 2^+) = 0.46 \pm 0.04 e^2\text{b}^2$ , indicating that there is no unexpected enhancement of the  $B(E2 : 0^+_{\text{g.s.}} \rightarrow 2^+)$  values in Te isotopes below the midshell. The result is compared to and discussed in the framework of large-scale shell-model calculations.

DOI: [10.1103/PhysRevC.91.061304](https://doi.org/10.1103/PhysRevC.91.061304)

PACS number(s): 21.10.Tg, 21.60.Cs, 27.60.+j

**Introduction.** The region near the  $N = Z$  line just above the large shell gap at  $^{100}\text{Sn}$  is well established as a testing ground for understanding the complex nuclear shell structure. In addition to the shell effects, an enhanced interplay between nucleons in this region might be expected since the protons and neutrons partially occupy the same quantum orbitals near the Fermi level.

The validity of the shell model far from stability can be tested in several ways. Ground-state masses and the energies of excited states are two important observables. Intense experimental activities and the advent of new accelerator and detector technologies have enabled us to extend the mass measurements and energy spectroscopy towards the  $N = Z$  line near  $A = 100$ . Still, more work is needed to map out single-particle and binding energies in the region. A complementary way of probing the nuclear wave function and to test the theoretical models is to investigate transition rates between nuclear states. Lifetime and Coulomb excitation measurements of low-lying excited states in this region have already allowed us to test the theory by comparing transition probabilities predicted by, e.g., the nuclear shell model with experimental results.

Unexpected large experimental  $B(E2 : 0^+ \rightarrow 2^+)$  values of neutron-deficient  $^{50}\text{Sn}$  isotopes have triggered a discussion regarding the interpretation within the framework of large-scale shell-model calculations. Especially the potential importance of core excitations across the  $Z = 50$  shell gap has been discussed [1–4]. A recent result for the  $B(E2)$  value in  $^{104}\text{Sn}$  [5] showed a significantly lower  $B(E2)$  value compared to its heavier even-mass neighbors and seemed to confirm a robust  $N = Z = 50$  shell closure. However, other recent experiments [6,7] showed a more moderate reduction of the  $0^+_{\text{g.s.}} \rightarrow 2^+$  transition rate in  $^{104}\text{Sn}$  compared to  $^{106}\text{Sn}$  and the challenge to properly understand the role of proton excitations across the  $Z = 50$  shell closure remains.

Measurements of transition rates in the isotopic chain of  $^{52}\text{Te}$  serve the same function as in  $^{50}\text{Sn}$  in evaluating the validity of the shell model in the region, e.g., the role of core excitations. Calculating theoretical  $B(E2)$  values for Te isotopes is, however, an even bigger challenge than

for Sn, especially in the midshell, due to the larger model space. Compared to tin, the experimental information is less abundant in the isotopic chain of tellurium. While experimental  $B(E2)$  values of neutron-rich Te isotopes are well established with small statistical uncertainties [8–13], little was known experimentally below the neutron midshell until recently. Transition rates were measured with the Doppler shift attenuation method (DSAM) as well as with the recoil distance Doppler shift method (RDDS) in the case of  $^{118}\text{Te}$  [14,15] and by using the RDDS technique for  $^{114}\text{Te}$  [16]. More recently, an important step in establishing the experimental values close to the  $N = Z$  line was achieved by measuring the lifetime in  $^{108}\text{Te}$  [17]. That measurement was made possible by combining the sensitive recoil-decay-tagging technique with a differential plunger. The predictions from standard shell-model calculations based on the CD-Bonn interaction were able to reproduce the experimental data. In this work we present a lifetime measurement of the first excited  $2^+$  state in  $^{112}\text{Te}$ . The result is interpreted in the framework of a large-scale shell-model calculation.

### I. EXPERIMENTAL DETAILS

**Experimental details.** The excited states in the  $^{112}\text{Te}$  nucleus were populated by the fusion-evaporation reaction  $^{58}\text{Ni}(^{58}\text{Ni}, 4p)$  at a beam energy of 250 MeV at the Accelerator Laboratory of the Department of Physics at the University of Jyväskylä (JYFL), Finland. The experimental setup used for the lifetime determination consisted of the Differential Plunger for Unbound Nuclear States (DPUNS) [18] in combination with the Jurogam II array [19,20] which comprised 15 Phase-I type and 24 segmented clovers from the previous Euroball array arranged in four rings, resulting in a photopeak efficiency of  $\sim 6\%$  at 1.3 MeV  $\gamma$ -ray energy. The plunger consisted of a  $^{58}\text{Ni}$  target foil of  $1.05 \text{ mg/cm}^2$  thickness coupled together with a  $1.2\text{-mg/cm}^2$  Mg degrader foil. The shift in velocity for the reaction products was used to distinguish  $\gamma$  rays emitted before and after the degrader, respectively, by their different Doppler-shifted energies. The RITU gas-filled recoil separator [21] was used to separate the recoils produced in the

reaction from the incoming beam particles. The selection of the recoil events was done by means of the energy deposited in the multiwire proportional counter (MWPC) and by the time-of-flight of the recoils measured between the MWPC gas detector and the double-sided silicon strip detectors of the focal plane detector system GREAT [22], where the recoils were implanted. Gamma rays in coincidence with these recoils were selected for the lifetime analysis. The off-line data were sorted by using the GRAIN software package [23] while the resulting  $\gamma$  matrices were analyzed with the RADWARE tools [24].

For the determination of the lifetime of the  $2^+$  state in  $^{112}\text{Te}$  a total of 11 plunger (target-to-degrader) distances were measured, ranging from 62 to 936  $\mu\text{m}$ , covering a lifetime range from approximately 2 to 80 ps.

*Method and results.* The lifetime determination of the  $2^+$  state at 689 keV [25,26] has been performed following the principles of the RDDS method [27–29] and the differential decay curve method [30] has been employed for the analysis. The intensity of both components of  $\gamma$  rays (shifted and degraded) has been obtained by calculating the areas of both peaks in the spectrum obtained from a  $\gamma$ - $\gamma$  matrix when a gate on the shifted component of the  $4^+ \rightarrow 2^+$  transition at 787 keV is imposed. Only the rings placed at  $133.6^\circ$  and  $157.6^\circ$  (tapered detectors) have been considered to build the  $\gamma$ - $\gamma$  matrices as the Doppler shift in energy of  $\gamma$  rays detected in the rings composed by clover detectors (located at  $104.5^\circ$  and  $75.5^\circ$ ) is not large enough to distinguish both components. Spectra obtained after gating at six distances in the sensitivity region are shown in Fig. 1.

The lifetime of the  $2^+$  state has been obtained by using the following relation:

$$\tau_i(d) = \frac{I_s^B I_d^A(d)}{\frac{d}{dx} I_s^B I_s^A(d)} \frac{1}{v}, \quad (1)$$

where  $I_s^B I_d^A$  and  $\frac{d}{dx} I_s^B I_s^A$  are the intensity of the degraded component and the derivative of the shifted component of the  $2^+ \rightarrow 0^+$   $\gamma$ -ray line, respectively, when a gate on the shifted component of the  $4^+ \rightarrow 2^+$   $\gamma$ -ray line at 787 keV is applied and  $v$  is the velocity of the recoils,  $v/c = 0.044(1)$ . To calculate the derivative of the shifted component with accurate uncertainties the APATHIE code [31] has been used. In Fig. 2 are shown the intensity of the degraded component ( $I_s^B I_d^A$ ) as well as the intensity of the shifted component ( $I_s^B I_s^A$ ) of the  $2^+ \rightarrow 0^+$   $\gamma$ -ray line as a function of the distance. Accordingly, the distances in which the slope of the fitted curve is well defined have been selected for the lifetime determination, going from 167 to 377  $\mu\text{m}$ . The lifetime values obtained by considering those distances are plotted in Fig. 2. It can be seen how the value obtained is practically constant with the distance indicating that there is no problem with side-feeding into the  $2^+$  state. The lifetime value extracted from the analysis is  $\tau = 5.7 \pm 0.5$  ps.

The reduced transition probability,  $B(E2; 0_{\text{g.s.}}^+ \rightarrow 2^+)$  (in  $e^2 b^2$ ), can be deduced from the lifetime of the excited state by:

$$B(E2 \uparrow) = 5 \left[ \frac{8.1766 \times 10^{-2}}{E^5 \tau (1 + \alpha)} \right], \quad (2)$$

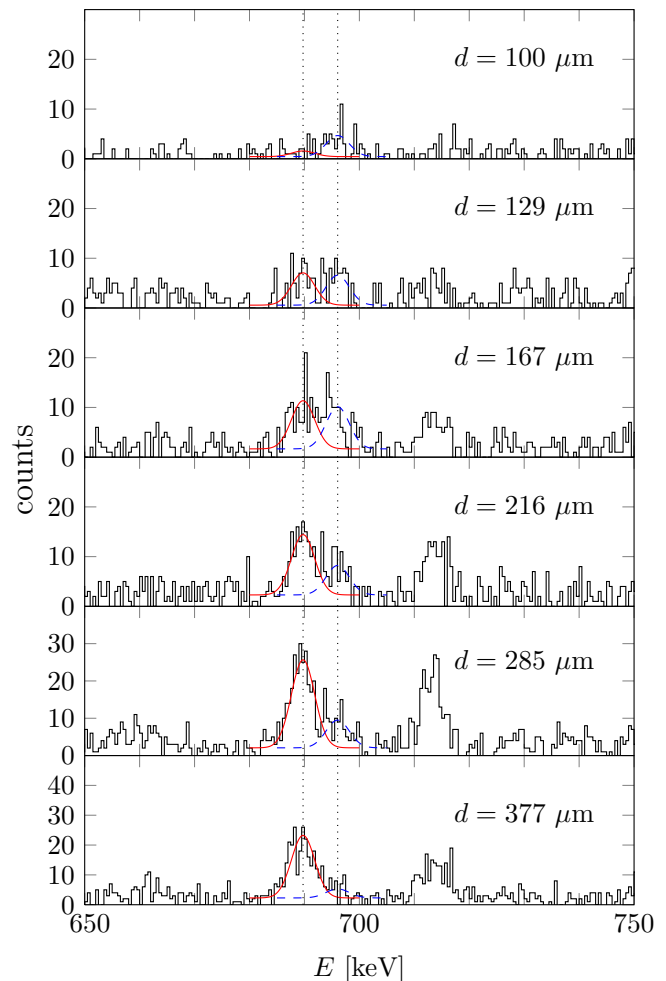


FIG. 1. (Color online) Spectra of the  $2^+ \rightarrow 0^+$  transition in  $^{112}\text{Te}$  obtained by gating on the 787-keV ( $4^+ \rightarrow 2^+$ ) transition for six plunger distances. The dashed (blue) and continuous (red) lines correspond to the shifted and degraded components at 689 and 696 keV, respectively.

where  $\alpha$  is the total conversion coefficient ( $\alpha = 3.47 \times 10^{-3}$ ),  $E$  is the transition energy in MeV, and  $\tau$  is the lifetime of the state in ps. The measured lifetime for the  $2^+$  state in  $^{112}\text{Te}$  corresponds to a reduced transition rate of  $B(E2 \uparrow) = 0.46 \pm 0.04 e^2 b^2 = 144 \pm 13 \text{ W.u.}$

*Discussion.* In the following discussion, we have compared the experimental data on  $E2$  transition probabilities for Te isotopes with the results of state-of-the-art shell-model calculations. The shell model has been shown to be rather successful in describing the structure and transition properties of nuclei in this region which involves the neutron and proton orbitals  $g_{7/2}$ ,  $d_{5/2}$ ,  $d_{3/2}$ ,  $s_{1/2}$ , and  $h_{11/2}$  [1,5,17,32–39].

The large shell-model space required makes the calculations very demanding, even on present-day high-performance computers. The tin isotopes are the longest chain that can be described by modern shell-model calculations. As for Te isotopes, the dimension for the midshell  $^{118}\text{Te}$  reaches  $10^{10}$  for which the diagonalization is still a very challenging numerical task. In our previous calculation for midshell Te isotopes [17],

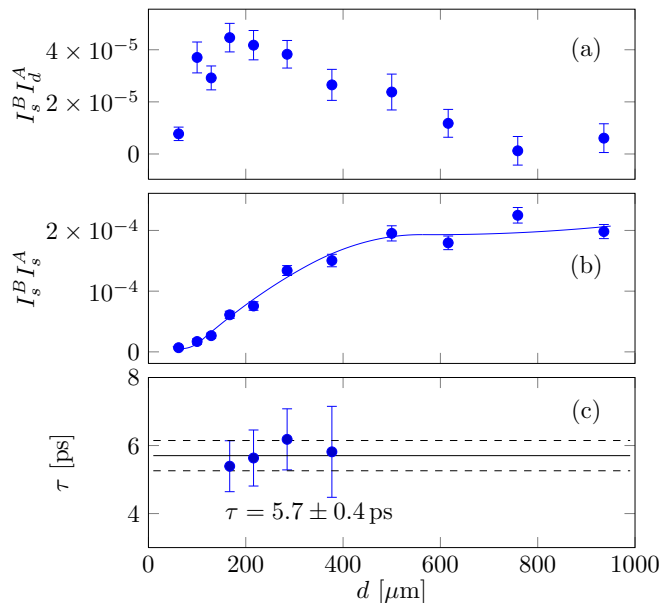


FIG. 2. (Color online) The upper two panels show the intensities of the degraded (a) and shifted (b) components of the  $\gamma$  rays depopulating the  $2^+$  state, as a function of the distance. The lifetime value obtained in the present measurement for the sensitive region is shown in panel (c).

we had restricted the maximum number of neutrons to four that could be excited from below the Fermi surface to the  $h_{11/2}$  subshell due to limited computation power. No proton excitation to  $h_{11/2}$  was allowed. A renormalized CD-Bonn potential [40] was used. The results agreed reasonably well with available experimental data. In Fig. 3 the experimental data on  $B(E2; 0^+_{\text{g.s.}} \rightarrow 2^+)$  in tellurium isotopes including the new result on  $^{112}\text{Te}$  are compared to the most recent shell-model calculations we have carried out. In comparison to

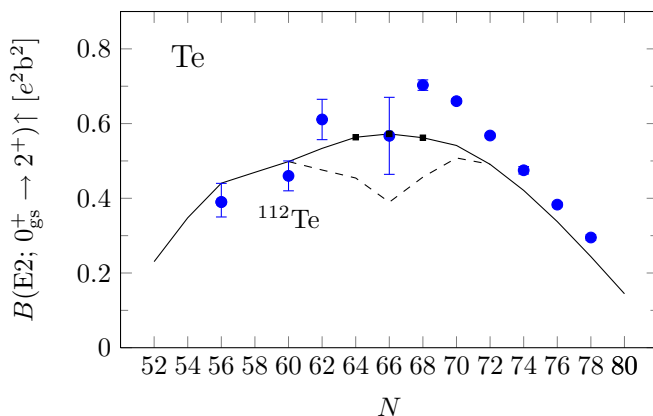


FIG. 3. (Color online) Comparison of the theoretical and experimental  $B(E2; 0^+_{\text{g.s.}} \rightarrow 2^+)$  values for the Te isotopic chain. The solid line corresponds to the calculation in which the full model space ( $g_{7/2}$ ,  $d_{5/2}$ ,  $d_{3/2}$ ,  $s_{1/2}$ , and  $h_{11/2}$ ) has been considered for all nuclei except  $^{116-120}\text{Te}$  (marked by small solid squares) while the dashed line represents the calculation in the smaller space, see the main text for more details.

our previous calculation, we are now able to treat the midshell Te isotopes in a much larger space, which reduces significantly the theoretical uncertainties as induced by the model space truncation. Moreover, the monopole interaction of the  $T = 1$  channel has been optimized, which gives a precise description on the properties of the ground and low-lying states in Sn isotopes [41]. The single-particle energies for  $g_{7/2}$  and  $d_{5/2}$  are set to be  $\varepsilon_{\text{sp}}(g_{7/2}) = 0$  and  $\varepsilon_{\text{sp}}(d_{5/2}) = 172$  keV [42]. The rest is determined by fitting to experimental data.

Two sets of calculations are presented in Fig. 3: In the first set, we have done calculations by restricting the maximum dimension to around  $10^9$ . Within that restriction, we can do full model-space calculations for  $N = 52-60$  and  $74-82$  and truncated calculations for  $N = 62-72$ , among which for  $N = 62, 64, 66$ , and  $68$  we allow a maximum of 4 particles (protons and neutrons) that can be excited to  $h_{11/2}$ , for  $N = 70$  a maximum of 6 particles, and for  $N = 72$  a maximum of 10 particles. In the second set, we have done calculations with maximal dimension up to around  $5 \times 10^9$  with the help of the new supercomputer at KTH that has been made available recently. This allows us to do full calculations for Te isotopes with  $N = 52-62$  and  $N = 70-82$  with a maximum of 8 particles excited to  $h_{11/2}$  for midshell  $^{116-120}\text{Te}$ . We have also done calculations by allowing at most 6 particles that can be excited to  $h_{11/2}$  for  $^{116-120}\text{Te}$ , giving values very close to the results shown in the figure, indicating that the  $E2$  calculation may have converged in the present truncation. It is beyond the scope of the present paper, but we may be able to carry out full shell-model calculations for all Te isotopes in the near future with further optimization of the code. The  $B(E2)$  value is calculated as  $B(E2; 0^+ \rightarrow 2^+) = (e_p M_p + e_n M_n)^2$  where we take effective charges  $e_p = 1.5 e$  and  $e_n = 0.8 e$  as were employed in Ref. [17]. Here  $M_p$  and  $M_n$  are the proton and neutron transition matrix elements, respectively. The possible isospin dependence of the effective charges is not taken into account here.

The model prediction agrees rather well with the new data point for  $^{112}\text{Te}$ . The  $B(E2)$  value for  $^{110}\text{Te}$  is still a missing point from the experimental point of view and work is planned to measure lifetimes in that isotope. The  $B(E2)$  values for both  $^{108,112}\text{Te}$  as predicted by the new calculation are slightly smaller in comparison to our previous results as presented in Ref. [17] and are even closer to experimental data. Moreover, there is no indication for enhanced  $E2$  transitions in  $^{108,112}\text{Te}$  relative to the corresponding isotopes on the right-hand side of the plot (Fig. 3). This may suggest that the  $^{100}\text{Sn}$  core is rather robust for all Te isotopes. As can be seen from the figure, the present calculations for midshell Te isotopes are quite sensitive to the filling of both the proton and neutron  $h_{11/2}$  subshells. A sudden dip is seen in the first set of calculations. On the other hand, both the proton ( $M_p$ ) and neutron ( $M_n$ ) transition matrix elements are enhanced when one goes from the first to the second set of large-scale calculations. This is particularly true for the midshell  $^{118}\text{Te}$ . The latter calculation coincides with the available experimental data at  $^{118}\text{Te}$  but the experimental uncertainty is still large. With our current choice of effective charges the theoretical values above midshell slightly underestimate the available data. It may be interesting to mention that the steepness of the parabolic curve of the

$B(E2)$  systematics shown in Fig. 3 is mainly driven by the neutron transition matrix elements, which means that a better description of the midshell nuclei may be obtained if the neutron effective charge is larger than that we assumed. It can be of great interest to pin down the uncertainties for the  $E2$  transitions of midshell Te isotopes, which may be helpful in clarifying the role played by  $h_{11/2}$  and neighboring orbitals in those nuclei.

*Summary.* The lifetime of the  $2^+$  excited state in the neutron-deficient nucleus  $^{112}\text{Te}$  has been measured by using the recoil distance Doppler shift technique. The value deduced for the reduced transition probability,  $B(E2; 0_{\text{g.s.}}^+ \rightarrow 2^+) = 0.46 \pm 0.04 e^2\text{b}^2$ , has been discussed in terms of new shell-model calculations which consider a large valence space allowing particle excitations to the  $h_{11/2}$  orbital.

*Acknowledgments.* This work was supported by the Swedish Research Council under Grants No. 826-2013-2109, No. 621-2012-3805, and No. 621-2013-4323; by the EU 7th Framework Programme, “Integrating Activities–Transnational Access,” project No. 262010 (ENSAR); by the Academy of Finland under the Finnish Centre of Excellence Programme (Nuclear and Accelerator Based Physics Programme at JYFL); by the STFC through a standard grant (Grant No. EP/E02551X/1; D.M.C. and M.J.T.); a Rolling grant (Grant No. ST/J000159/1); and a consolidated grant (Grant No. ST/L005794/1). The calculations were performed on resources provided by the Swedish National Infrastructure for Computing (SNIC) at NSC in Linköping and PDC at KTH, Stockholm. The authors acknowledge the support of GAMMAPOOL for the loan of the Jurogam detectors.

- 
- [1] A. Banu *et al.*, *Phys. Rev. C* **72**, 061305 (2005).  
 [2] J. Cederkäll *et al.*, *Phys. Rev. Lett.* **98**, 172501 (2007).  
 [3] C. Vaman *et al.*, *Phys. Rev. Lett.* **99**, 162501 (2007).  
 [4] A. Ekström *et al.*, *Phys. Rev. Lett.* **101**, 012502 (2008).  
 [5] G. Guastalla *et al.*, *Phys. Rev. Lett.* **110**, 172501 (2013).  
 [6] V. M. Bader *et al.*, *Phys. Rev. C* **88**, 051301(R) (2013).  
 [7] P. Doornenbal *et al.*, *Phys. Rev. C* **90**, 061302 (2014).  
 [8] J. R. Terry *et al.*, *AIP Conf. Proc.* **1090**, 337 (2009).  
 [9] C. Mihai *et al.*, *Phys. Rev. C* **81**, 034314 (2010).  
 [10] C. Doll *et al.*, *Nucl. Phys. A* **672**, 3 (2000).  
 [11] J. R. Vanhoy *et al.*, *Phys. Rev. C* **69**, 064323 (2004).  
 [12] S. F. Hicks *et al.*, *Phys. Rev. C* **86**, 054308 (2012).  
 [13] S. F. Hicks, J. R. Vanhoy, and S. W. Yates, *Phys. Rev. C* **78**, 054320 (2008).  
 [14] A. A. Pasternak *et al.*, *Eur. Phys. J. A* **13**, 435 (2002).  
 [15] C. Mihai *et al.*, *Phys. Rev. C* **83**, 054310 (2011).  
 [16] O. Möller *et al.*, *Phys. Rev. C* **71**, 064324 (2005).  
 [17] T. Bäck *et al.*, *Phys. Rev. C* **84**, 041306(R) (2011).  
 [18] M. J. Taylor *et al.*, *Nucl. Instrum. Methods A* **707**, 143 (2013).  
 [19] F. Beck *et al.*, *Prog. Part. Nucl. Phys.* **28**, 443 (1992).  
 [20] C. Beausang and J. Simpson, *J. Phys. G* **22**, 527 (1996).  
 [21] M. Leino *et al.*, *Nucl. Instrum. Methods B* **99**, 653 (1995).  
 [22] R. Page *et al.*, *Nucl. Instrum. Methods B* **204**, 634 (2003).  
 [23] P. Rahkila, *Nucl. Instrum. Methods A* **595**, 637 (2008).  
 [24] D. C. Radford, *Nucl. Instrum. Methods A* **361**, 297 (1995).  
 [25] E. S. Paul *et al.*, *Phys. Rev. C* **75**, 014308 (2007).  
 [26] E. S. Paul *et al.*, *Phys. Rev. C* **50**, 698 (1994).  
 [27] T. K. Alexander and J. S. Foster, *Adv. Nucl. Phys.* **10**, 197 (1978).  
 [28] P. Petkov *et al.*, *Nucl. Instrum. Methods A* **431**, 208 (1999).  
 [29] P. Petkov *et al.*, *Nucl. Instrum. Methods A* **560**, 564 (2006).  
 [30] A. Dewald, S. Harissopulos, and P. von Brentano, *Z. Phys. A* **334**, 163 (1989).  
 [31] F. Seiffert (unpublished).  
 [32] K. Sieja, G. Martínez-Pinedo, L. Coquard, and N. Pietralla, *Phys. Rev. C* **80**, 054311 (2009).  
 [33] G. S. Simpson *et al.*, *Phys. Rev. Lett.* **113**, 132502 (2014).  
 [34] M. G. Procter *et al.*, *Phys. Lett. B* **704**, 118 (2011).  
 [35] M. G. Procter *et al.*, *Phys. Rev. C* **86**, 034308 (2012).  
 [36] M. G. Procter *et al.*, *Phys. Rev. C* **87**, 014308 (2013).  
 [37] T. Bäck *et al.*, *Phys. Rev. C* **87**, 031306(R) (2013).  
 [38] H. Jiang *et al.*, *Phys. Rev. C* **88**, 044332 (2013).  
 [39] M. Saxena *et al.*, *Phys. Rev. C* **90**, 024316 (2014).  
 [40] M. Hjorth-Jensen *et al.*, *Phys. Rep.* **261**, 125 (1995).  
 [41] C. Qi and Z. X. Xu, *Phys. Rev. C* **86**, 044323 (2012).  
 [42] I. Darby *et al.*, *Phys. Rev. Lett.* **105**, 162502 (2010).